J Fluoresc (2012) 22:1357–1370
DOI 10.1007/s10895-012-1075-8

ORIGINAL PAPER

Aromatic Chromophore-Tethered Schiff Base Ligands and Their Iron(III)/Chromium(III) Salen and Saloph Capped Complexes

Aslihan Yilmaz Obali · Halil Ismet Ucan

Received: 29 December 2011 / Accepted: 30 May 2012 / Published online: 14 June 2012

Abstract Aromatic chromophores; pyrene, phenanthrene, anthracene, naphtalene and benzene-tethered Schiff base ligands and their iron(III)/chromium(III) Salen and Saloph capped complexes have been synthesized. Compounds have been characterized by means of FT-IR Spectroscopy, ^{1}H-NMR Spectroscopy, Magnetic Susceptibility, Elementel Analsis, TG/DTA measurements. Their fluorescence and absorbance properties have been investigated by Luminescence Spectroscopy and UV–vis Spectroscopy. Generally, ligands show an intense excimer fluorescence emissions in acetonitrile-methanol medium while iron(III) and chromium(III) complexes exhibit low fluorescence's. Intensity compared to ligands iron and chromium centers act as an extra chromophore that quench the pyrene, phenanthrene, anthracene, naphtalene and benzene molecules' singlet state. The mechanism of quenching is attributed to a iron (or chromium)-to-pyrene (or phenanthrene, anthracene, naphtalene and benzene) electronic energy transfer process.

Keywords Fluorescence · Schiff base · Salen · Saloph · Metal complexes

Introduction

Chromogenic or fluorogenic signaling is much more attractive due to their sensitivity and easiness of signal detection. Among the chromophores, pyrene, phenanthrene, anthracene, naphtalene compounds are most widely employed due to their relatively well exploited photophysical behaviors [1–4]. Fluorescent molecules for 3d transition series trivalent metal ions have been designed by means of a supramolecular approach: a pyrene fragment (the signalling subunit-chromophore) has been linked to Schiff base ligand (the receptor). Occurrence of the metal receptor interaction can be signalled through either quenching or enhancement of chromophore fluorescence. Where the receptor is able to promote the one electron resulting in oxidation of the metal, quenching takes place through a photoinduced metal-to-chromophore electron transfer mechanism. There are extensive investigations toward the characterization of chromophores including crown ether, calixarene, and cyclodextrin derivatives with naphthalene, anthracene, or pyrene chromophore. Recently, most of the chromophores designed for metal ions operate by a photoinduced electron transfer mechanism [5–15]. In a classic example from the de Silva group [8–11], the binding component of the sensor is *N*-(9-anthrylmethyl)-18-azacrown-6. The quenching of singlet and triplet excited states of aromatic hydrocarbons by transition metal ions and their coordination complexes is the most popular subject of intense investigations. A great deal of attention has been devoted to the design and the synthesis of transition metal complexes of chromophore-tethered ligands. These metallosystems have found applications of paramount interest in many areas such as optical sensing, photocatalysis, DNA cleavage. We have designed novel chromophore-tethered ligands and investigated the quenching effect of Fe(III) and Cr(III) on those compounds.

Metal complexes of the 'Salen-type' ligands have been considered as interesting species in many fields of chemical research because of some specific properties. Fe-Salen complexes have been extensively studied in the solid state and in solution [16–18]

Tonami et al.[19] show a synthesis of a soluble polyphenol by oxidative polymerization of bisphenol-A using Fe-Salen

A. Y. Obali (✉) · H. I. Ucan
Department of Chemistry, Science Faculty, Selcuk University, Campus,
42075 Konya, Turkey
e-mail: aslihanyilmazobali@gmail.com

complex as catalyst. Barone et al. [20] show a catalytic activity toward the blend oxidation of hydrocarbons and undergo electron transfer reactions, mimicking the catalytic functions of peroxidases. Herein, we have reported the syntheses of novel aromatic chromophore group-tethered carboxylic acid ligands and their [Fe(III)/Cr(III) (Salen/Saloph)] capped complexes. The reaction of [{Fe(Salen)}$_2$O] with carboxylic acids has been described by Wollmann and Hendrickson [21]. Koc and Ucan have reported the synthesis and characterization of 1,3,5-tricarboxylato bridges with [Fe(III) (Salen/Saloph)] [22]. We have preferred iron and chromium complexes because they are biologically significant at all the levels of living organisms [23]. Chromium(III) complexes of Salen type Schiff bases have been found to enhance insulin activity. And also, various metal-Salen complexes such as manganese(III), chromium(III) and nickel(II)-Salen complexes have been used for the epoxidation of olefins [24–27].

Experimental

Materials and Methods

4-Aminobenzoic acid, benzaldehyde, 2-naphtaldehyde, 9-anthraldehyde, 9-phenanthrenecarbaldehyde, 1-pyrenecarbaldehyde and all other reagents were purchased from Alfa Aesar, Sigma Aldrich, Merck and used without further purification. [{Fe(Salen)}$_2$O], [{Fe(Saloph)}$_2$O], [{Cr(Salen)}$_2$O] and [{Cr(Saloph)}$_2$O] were prepared according to previously published methods [28–30].

^{1}H-NMR spectra were taken using a Bruker 400-MHz Spectrometer. IR spectra were recorded using a Perkin Elmer Spectrum 100 FT-IR spectrometer. Melting points were determined by Büchi Melting Point B-540 instrument. Elemental analyses were carried out using a LECO-CHNS-932 elementel analyser. pH values were measured through a

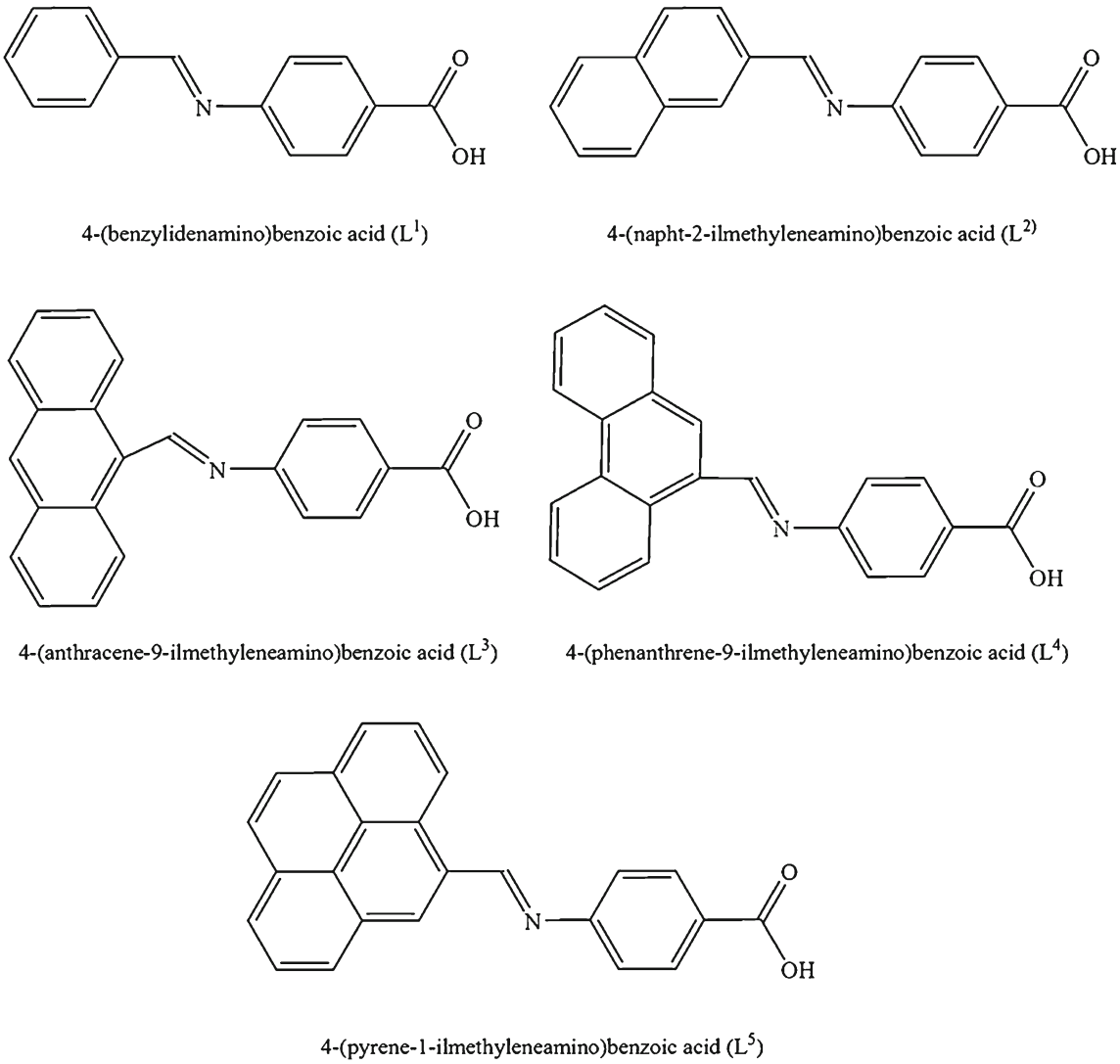

Fig. 1 The structures of different tip Schiff base ligands

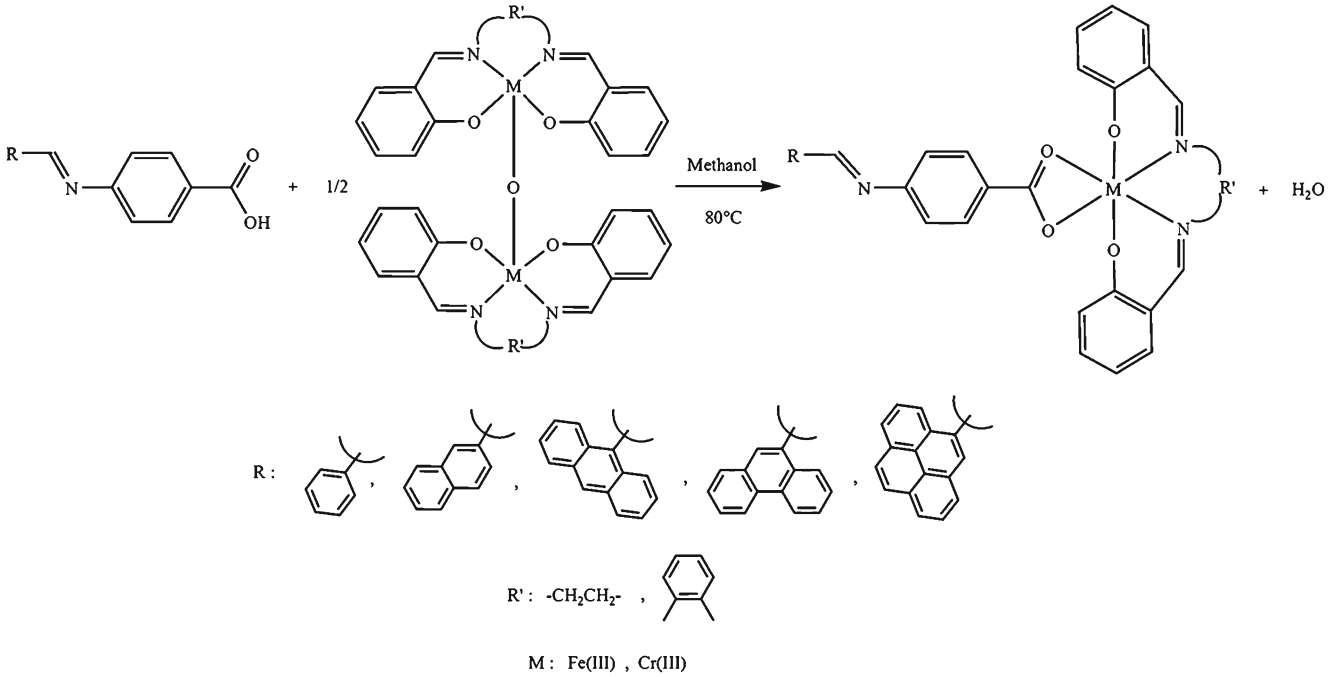

Fig. 2 Complexation scheme of [Fe(Salen)L^n], [Fe(Saloph)L^n], [Cr(Salen)L^n] and [Cr(Saloph)L^n] (n stands for 1, 2, 3, 4, 5)

Table 1 Characteristic FT-IR values of the ligands and complexes

	Compounds	C = N $_{imine}$	C = O	COO^-	OH $_{acid}$	ArCH	ArCH	C-C $_{aromatic}$	C-H $_{aliphatic}$
1	L^1	1677	–	1288	2875	3150	851	1449	2548
2	[Fe(Salen)L^1]	1631	1677	1291	–	3229	785	1444	2914
3	[Fe(Saloph)L^1]	1603	1578	1317	–	3339	757	1444	3015
4	[Cr(Salen)L^1]	1623	1681	1398	–	3322	760	1470	2676
5	[Cr(Saloph)L^1]	1598	1676	1385	–	3015	743	1398	2921
6	L^2	1684	–	1288	2920	3005	864	1448	2530
7	[Fe(Salen)L^2]	1624	1644	1286	–	3110	748	1464	2905
8	[Fe(Saloph)L^2]	1601	1635	1295	–	3053	749	1463	2914
9	[Cr(Salen)L^2]	1621	1684	1398	–	2919	740	1470	2498
10	[Cr(Saloph)L^2]	1595	1682	1385	–	3055	740	1458	2500
11	L^3	1678	–	1285	3155	3245	876	1419	2533
12	[Fe(Salen)L^3]	1621	1637	1288	–	3147	869	1441	2934
13	[Fe(Saloph)L^3]	1581	1604	1313	–	3150	872	1461	2987
14	[Cr(Salen)L^3]	1623	1666	1338	–	3051	873	1443	2923
15	[Cr(Saloph)L^3]	1601	1666	1399	–	3000	847	1457	2929
16	L^4	1685	–	1291	3150	3240	854	1426	2551
17	[Fe(Salen)L^4]	1589	1631	1296	–	3227	863	1470	2864
18	[Fe(Saloph)L^4]	1581	1604	1313	–	3150	853	1461	2987
19	[Cr(Salen)L^4]	1597	1685	1291	–	3033	855	1476	2988
20	[Cr(Saloph)L^4]	1530	1595	1291	–	3064	859	1457	2801
21	L^5	1675	–	1291	3047	2807	840	1426	2538
22	[Fe(Salen)L^5]	1628	1644	1301	–	3025	851	1434	2907
23	[Fe(Saloph)L^5]	1576	1603	1305	–	3012	854	1459	2845
24	[Cr(Salen)L^5]	1624	1674	1315	–	3040	839	1414	2715
25	[Cr(Saloph)L^5]	1589	1623	1291	–	3048	848	1401	2912

Orion Expondoble Ion Analyzer EA 940 pH meter. Magnetic susceptibilities of metal complexes were determined using a Sheerwood Scientific MX Gouy magnetic susceptibility apparatus using the Gouy method with $Hg[Co(SCN)_4]$ as calibrant. The thermal analyses were performed on Setaram SETSYS Evolution TGA/DTG DSC model. The DTA and TG curves were obtained at the heating rate of 10 °C/min. In all cases, the 40–900 °C temperature range was studied under a dry nitrogen atmosphere. UV–vis spectra were recorded on Perkin Elmer Lambda 25 UV–vis Spectrometer. The fluorescence measurements were performed using a Perkin Elmer LS 55 Luminescence Spectrometer.

Preparation of Ligands and Their Metal Complexes

Aromatic chromophore-tethered Sciff base ligands; 4-(benzylidenamino)benzoic acid, 4-(napht-2-ilmethyleneamino)benzoic acid,4-(anthracene-9-ilmethyleneamino)benzoic acid, 4-(phenanthrene-9-ilmethyleneamino)benzoic acid, 4-(pyrene-1-ilmethyleneamino)benzoic acid (L^5) were synthesized originally (Fig. 1). N,N'-bis(o-hydroxybenzylidene)ethylenediamine (Salen) and N,N'-bis(o-hydroxybenzylidene)-1,2-diaminobenzene (Saloph) compounds and their oxygen bridged Fe(III) and Cr(III) bridge complexes, $[\{FeSalen\}_2O]$, $[\{FeSalophen\}_2O]$, $[\{CrSalen\}_2O]$, $[\{CrSalophen\}_2O]$ are synthesized in accordance with the literature [31].

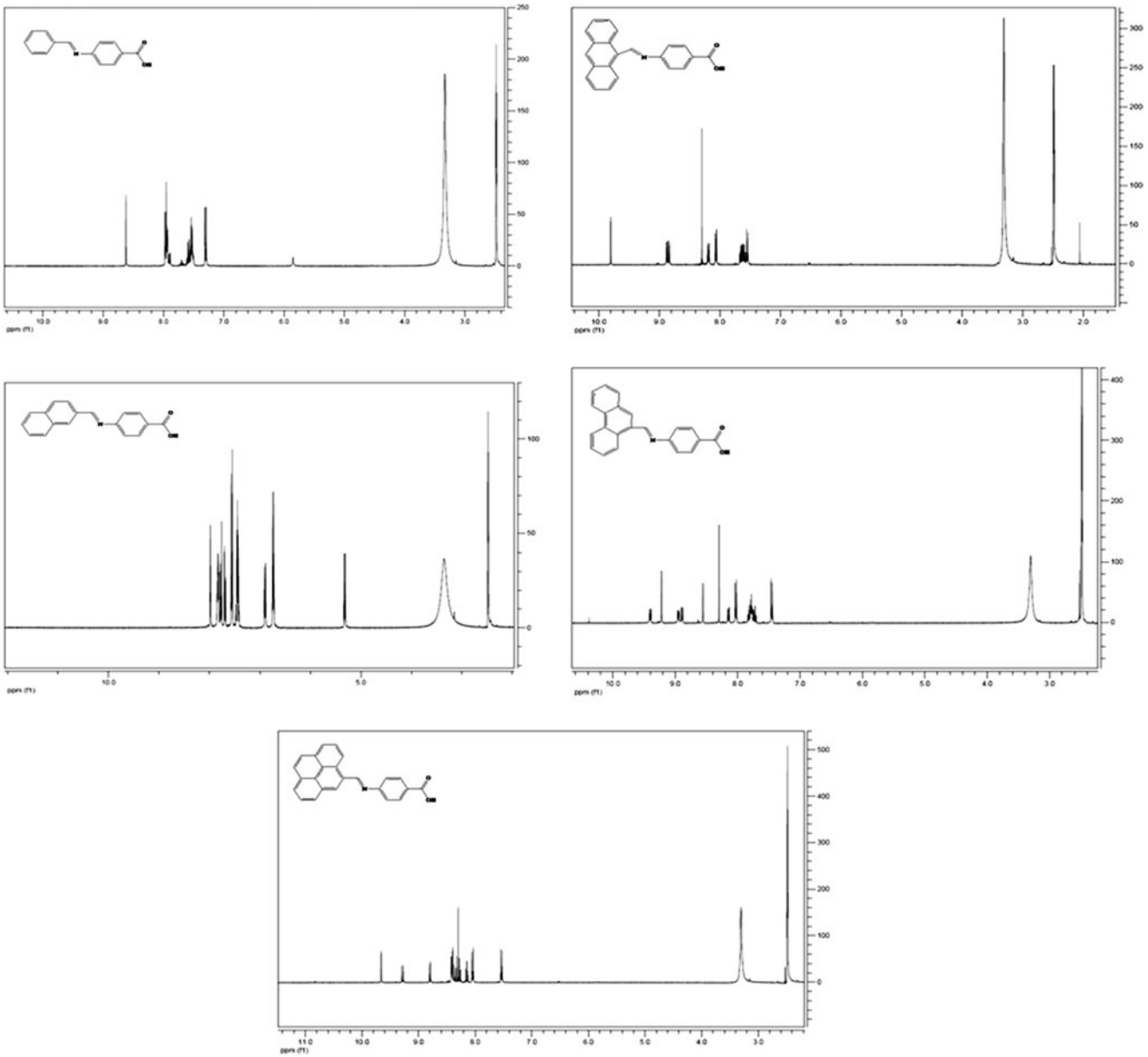

Fig. 3 ^{1}H-NMR spectra of the ligands; 4-(benzylidenamino)benzoic acid, 4-(napht-2-ilmethyleneamino)benzoic acid, 4-(anthracene-9-ilmethyleneamino) benzoic acid, 4-(phenanthrene-9-ilmethyleneamino)benzoic acid, 4-(pyrene-1-ilmethyleneamino)benzoic acid in D6-DMSO

General Procedure for Syntheses of Schiff Base Ligands

To a stirred solution of (1 mmol) aldehyde (benzaldehyde for L^1, 2-naphtaldehyde for L^2, 9-anthraldehyde for L^3, 9-phenanthrene carbaldehyde for L^4, 1-pyrene carbaldehyde for L^5) in 10 mL acetonitrile, was added dropwise a solution of (1.2 mmol) 4-aminobenzoic acid in 10 mL acetonitrile. The reaction mixture was stirred at room temperature for 24 h. The resulting substance was filtered, washed with cold ethanol and acetonitrile, recrystallized from methanol. The crystals were filtered and dried *in vacuo* (0.4 bar) at 60 °C.

4-(benzylidenamino)benzoic acid (L^1); Yield: % 67 (0.13 g), M.P. : 205 °C, FT-IR: 1,677 cm^{-1}(C = N), ^{1}H-NMR (DMSO-d6): δ 7.25–7.40 (d, 2H, -CH), 7.43–7.62 (m, 5H, (Ar)) ve 7.95 (d, 2H, -CH), 8.2 (d, 2H, -CH), 8.60 (s, ^{1}H, -HC = N-), λ_{ems}: 351.22 nm, Fluorescence Intensity: 867.72 (λ_{exc}: 242.71 nm), λ_{max}: 206 nm, A: 3.3474.

4-(napht-2-ilmethyleneamino)benzoic acid (L^2); Yield: % 53 (0.14 g), M.P.: 225 °C, FT-IR: 1,684 cm^{-1}(C = N), ^{1}H-NMR (DMSO-d6): δ 7.25–7.40 (d, 2H, -CH), 7.44–7.65 (m, 2H, (Ar)) ve 7.95–8.03 (d, 2H, -CH), 7.90–8.20 (d, 2H, (Ar)), 8.41 (s, 1H, -CH), 8.81 (s, 1H, -HC = N-), λ_{ems}: 297.65 nm, Fluorescence Intensity: 306.82 (λ_{exc}: 227.55 nm), λ_{max}: 248 nm, A: 2.537.

4-(anthracene-9-ilmethyleneamino)benzoic acid (L^3); Yield: % 64 (0.21 g), M.P.: 253 °C, FT-IR: 1,678 cm^{-1}(C = N), ^{1}H-NMR (DMSO-d6): δ 7.5–7.7 (m, 4 H, (Ar)), 7.55 (d, 2H, -CH) ve 8.1 (d, 2H, -CH), 8.2 (d, 2H, -CH), 8.3 (s, 1H, -CH), 8.8–8.9 (t, 4 H, -CH), 9.8 (s, 1H, -HC = N-), λ_{ems}: 300.63 nm, Fluorescence Intensity: 329.84 (λ_{exc}: 227.55 nm), λ_{max}: 253 nm, A: 3.3119.

4-(phenanthrene-9-ilmethyleneamino)benzoic acid (L^4); Yield: % 55 (0.18 g), M.P.: 256 °C, FT-IR: 1,685 cm^{-1}(C = N), ^{1}H-NMR (DMSO-d6): δ 7.43 (d, 1H) ve 8.0–8.1 (d, 1H), 7.7–7.85 (m, 6H, (Ar)), 8.15–8.2 (d, 1H) ve 8.86–8.90 (d, 1H), 8.3 (s, 1H, (Ar)), 8.55 (s, 1H, -HC = N-), 8.12–8.19 (d, 1H) ve 8.86–8.91 (d, 1H), 8.92–9.0 (d, 1H) ve 9.35–9.44 (d, 1H), Elementel analysis; Calculated (Found): C 81.23 (81.05), H 4.61 (4.52), N 4.30 (4.22), O 9.86 (10.11), λ_{ems}: 296.87 nm, Fluorescence Intensity: 369.79 (λ_{exc}: 227.55 nm), λ_{max}: 252 nm, A: 1.0832.

4-(pyrene-1-ilmethyleneamino)benzoic acid (L^5); Yield: % 46 (0.16 g), M.P.: 240 °C, FT-IR: 1,675 cm^{-1}(C = N), ^{1}H-NMR (DMSO-d6): δ 7.5 (d, 1H) ve 8.0–8.1 (d, 1H), 8.1–8.2 (t, 2H), 8.3 (s, 1H, (Ar)), 8.24–8.45 (m, 6H, (Ar)), 8.76–8.81 (d, 1H) ve 9.25–9.31 (d, 1H), 9.65–9.69 (s, 1H, -HC = N), Elementel analysis; Calculated (Found):C 82.52 (82.67), H 4.29 (4.52), N 4.01 (4.28), O 9.18 (8.52), λ_{ems}: 296.87 nm,

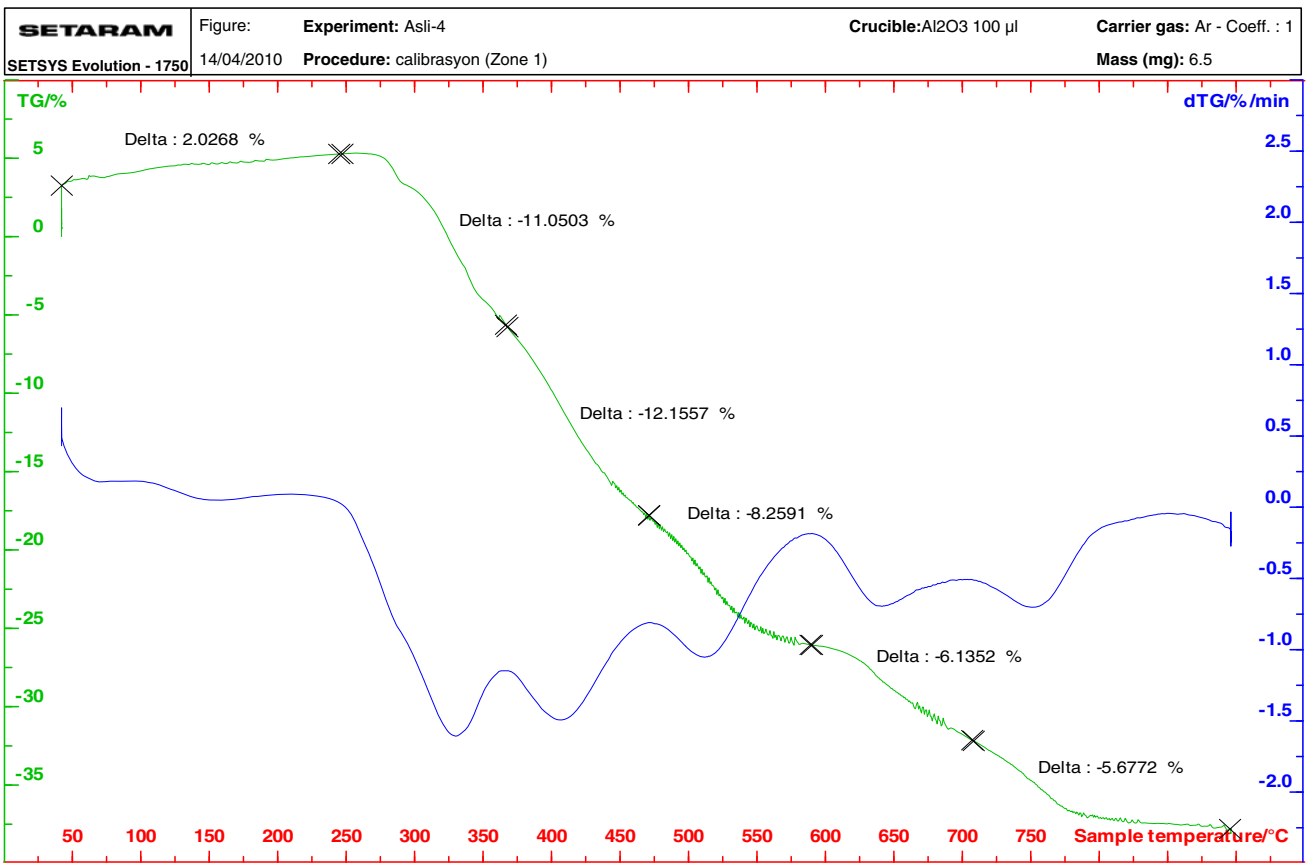

Fig. 4 TG/DTA diagram of [Fe(Saloph)L^3]

Fluorescence Intensity: 410.42 (λ_{exc}: 227.55 nm), λ_{max}: 241 nm, A: 2.4721.

General Procedure for Syntheses of Complexes

To the suspension of (0.40 mmol) [{Fe(Salen)}$_2$O] (or [{Fe(Saloph)}$_2$O], or [{Cr(Salen)}$_2$O], or [{Cr(Saloph)}$_2$O]) in 20 mL hot methanol, was added dropwise a solution of (0.80 mmol) L^n ligand in 20 mL hot methanol. The reaction mixture was refluxed at 50 °C for 36 h. The resulting substance was filtered, washed with hot methanol and diethyl ether, dried *in vacuo* (0.4 bar) at 60 °C.

For the Complexes of L^1 **[Fe(Salen)L^1];** Yield: % 53 (0.23 g), M.P.: 253 °C, FT-IR: 1,631 cm^{-1} (C = N), Color: Red, BM: 1.50, λ_{ems}: 342.81 nm, Fluorescence Intensity: 336.62, λ_{max}: 219 nm, A: 2.903, **[Fe(Saloph)L^1)];** Yield: % 62 (0.29 g), M.P.: 272 °C, FT-IR: 1,603 cm^{-1} (C = N), Color: Brown, BM: 1.68 λ_{ems}: 349.79 nm, Fluorescence Intensity: 464.7, λ_{max}: 295 nm, A: 3.0874, **[Cr(Salen)L^1)];** Yield: % 34 (0.14 g), M.P.: 288 °C, FT-IR: 1,623 cm^{-1} (C = N), Color: Green, BM: 3.55, λ_{ems}: 295.60 nm, Fluorescence Intensity: 245.87, λ_{max}: 200 nm, A: 1.4634, **[Cr(Saloph)L^1];** Yield: % 48 (0.22 g), M.P.: 287 °C, FT-IR: 1,598 cm^{-1} (C = N), Color: Green, BM: 3.23, λ_{ems}: 295.60 nm, Fluorescence Intensity: 236.49, λ_{max}: 200 nm, A: 1.8221.

(For the complexes of L^1 ligand, the fluorescence intensities were measured at λ_{exc}: 242.71 nm).

For the Complexes of L^2 **[Fe(Salen)L^2];** Yield: % 61 (0.25 g), M.P.: 268 °C, FT-IR: 1,624 cm^{-1} (C = N), Color: Brown, BM: 1.69, λ_{ems}: 300.20 nm, Fluorescence Intensity: 264.46, λ_{max}: 221 nm, A: 1.3493, **[Fe(Saloph)L^2];** Yield: % 68 (0.31 g), M.P.: 342 °C, FT-IR: 1,601 cm^{-1} (C = N), Color: Brown, BM: 1.70, λ_{ems}: 300.20 nm, Fluorescence Intensity: 232.14, λ_{max}: 219 nm, A: 0.6474, **[Cr(Salen)L^2];** Yield: % 35 (0.13 g), M.P.: 278 °C, FT-IR: 1,621 cm^{-1} (C = N), Color: Green, BM: 3.14, λ_{ems}: 297.13 nm, Fluorescence Intensity: 359.69, λ_{max}: 222 nm, A: 0.9533, **[Cr(Saloph)L^2];** Yield: % 56 (0.25 g), M.P.: 291 °C, FT-IR: 1,595 cm^{-1} (C = N), Color: Green, BM: 3.43, λ_{ems}: 301.73 nm, Fluorescence Intensity: 266.77, λ_{max}: 221 nm, A: 1.8605.

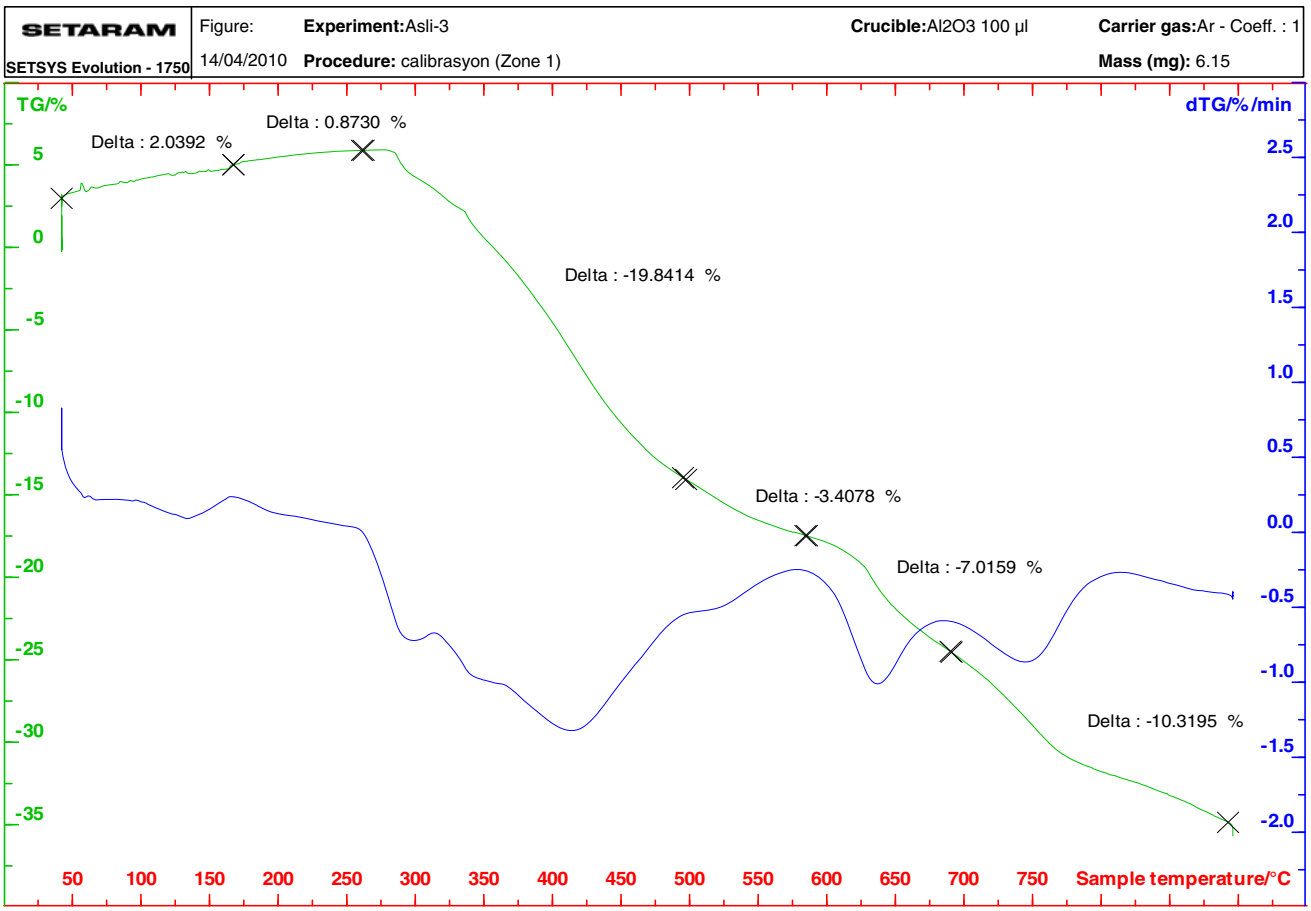

Fig. 5 TG/DTA diagram of [Fe (Saloph) L^4]

(For the complexes of L^2 ligand, the fluorescence intensities were measured at λ_{exc}: 227.55 nm).

For the Complexes of L^3 **[Fe(Salen)L^3];** Yield: % 68 (0.26 g), M.P.: 278 °C, FT-IR: 1,621 cm^{-1} (C = N), Color: Brown, BM: 1.97, λ_{ems}: 296.11 nm, Fluorescence Intensity: 526.96, λ_{max}: 253 nm, A: 1.0055, **[Fe(Saloph)L^3];** Yield: % 73 (0.32 g), M.P.: 301 °C, FT-IR: 1,581 cm^{-1} (C = N), Color: Brown, BM: 1.99, λ_{ems}: 299.69 nm, Fluorescence Intensity: 294.60, λ_{max}: 250 nm, A: 1.0902, **[Cr(Salen)L^3];** Yield: % 42 (0.16 g), M.P.: 325 °C, FT-IR: 1,623 cm^{-1} (C = N), Color: Yellow, BM: 3.68, λ_{ems}: 298.15 nm, Fluorescence Intensity: 367.90, λ_{max}: 255 nm, A: 1.4216, **[Cr (Saloph)L^3];** Yield: % 53 (0.24 g), M.P.: 345 °C, FT-IR: 1,601 cm^{-1} (C = N), Color: Yellow, BM: 3.70, λ_{ems}: 300.71 nm, Fluorescence Intensity: 265.26, λ_{max}: 255 nm, A: 3.321.

(For the complexes of L^3 ligand, the fluorescence intensities were measured at λ_{exc}: 227.56 nm).

For the Complexes of L^4 **[Fe(Salen)L^4];** Yield: % 72 (0.28 g), M.P.: 275 °C, FT-IR: 1,589 cm^{-1} (C = N), Color: Brown, BM: 1.97, λ_{ems}: 299.18 nm, Fluorescence Intensity: 147.62, λ_{max}: 250 nm, A: 0.5401, **[Fe(Saloph)L^4];** Yield: % 68 (0.31 g), M.P.: 293 °C, FT-IR: 1,581 cm^{-1} (C = N), Color: Brown, BM: 1.86, λ_{ems}: 299.18 nm, Fluorescence Intensity: 175.81, λ_{max}: 254 nm, A: 1.5255, **[Cr(Salen)L^4];** Yield: % 35 (0.13 g), M.P.: 334 °C, FT-IR: 1,597 cm^{-1} (C = N), Color: Green, BM: 3.16, λ_{ems}: 300.71 nm, Fluorescence Intensity: 150.62, λ_{max}: 207 nm, A: 3.5425, **[Cr(Saloph)L^4];** Yield: % 43 (0.19 g), M.P.: 399 °C, FT-IR: 1,530 cm^{-1} (C = N), Color: Green, BM: 3.26, λ_{ems}: 300.20 nm, Fluorescence Intensity: 176.06, λ_{max}: 203 nm, A: 2.6077.

(For the complexes of L^4 ligand, the fluorescence intensities were measured at λ_{exc}: 227.77 nm).

For the Complexes of L^5 **[Fe(Salen)L^5];** Yield: % 75 (0.14 g), M.P.: 293 °C, Color: Brown, BM: 1.84, FT-IR: 1,628 cm^{-1} (C = N), λ_{ems}: 299.18 nm, Fluorescence Intensity: 182.61, λ_{max}: 232 nm, A: 1.4992, **[Fe(Saloph)L^5];** Yield: % 67 (0.13 g), M.P.: 290 °C, FT-IR: 1,576 cm^{-1} (C = N), Color: Brown, BM: 1.58, λ_{ems}: 300.20 nm, Fluorescence Intensity: 177.69, λ_{max}: 238 nm, A: 1.2702, **[Cr (Salen)L^5];** Yield: % 31 (0.06 g), M.P.: 323 °C, FT-IR: 1,624 cm^{-1} (C = N), Color: Yellow, BM: 3.59, λ_{ems}: 298.67 nm, Fluorescence Intensity: 189.59, λ_{max}: 232 nm,

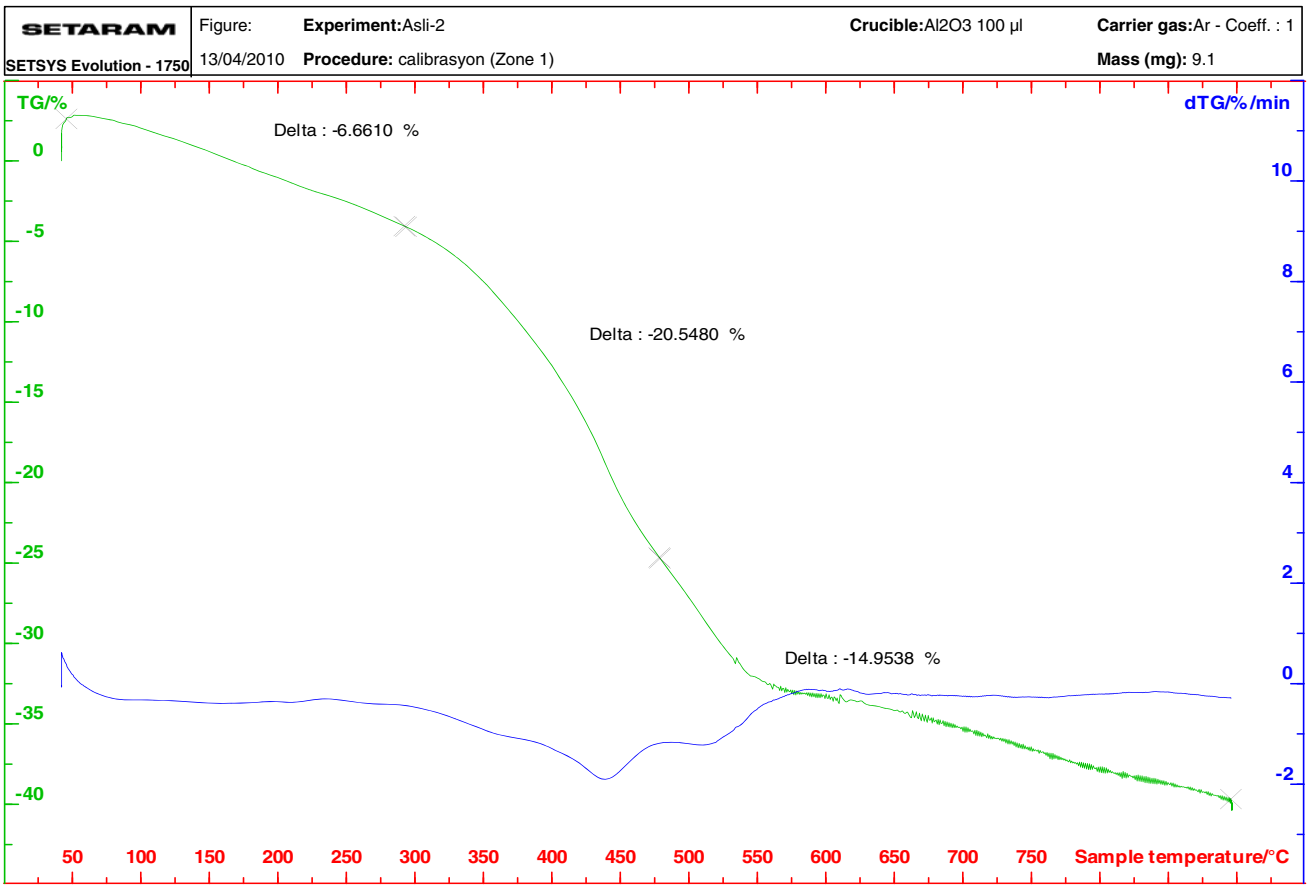

Fig. 6 TG/DTA diagram of [Cr (Salen) L^4]

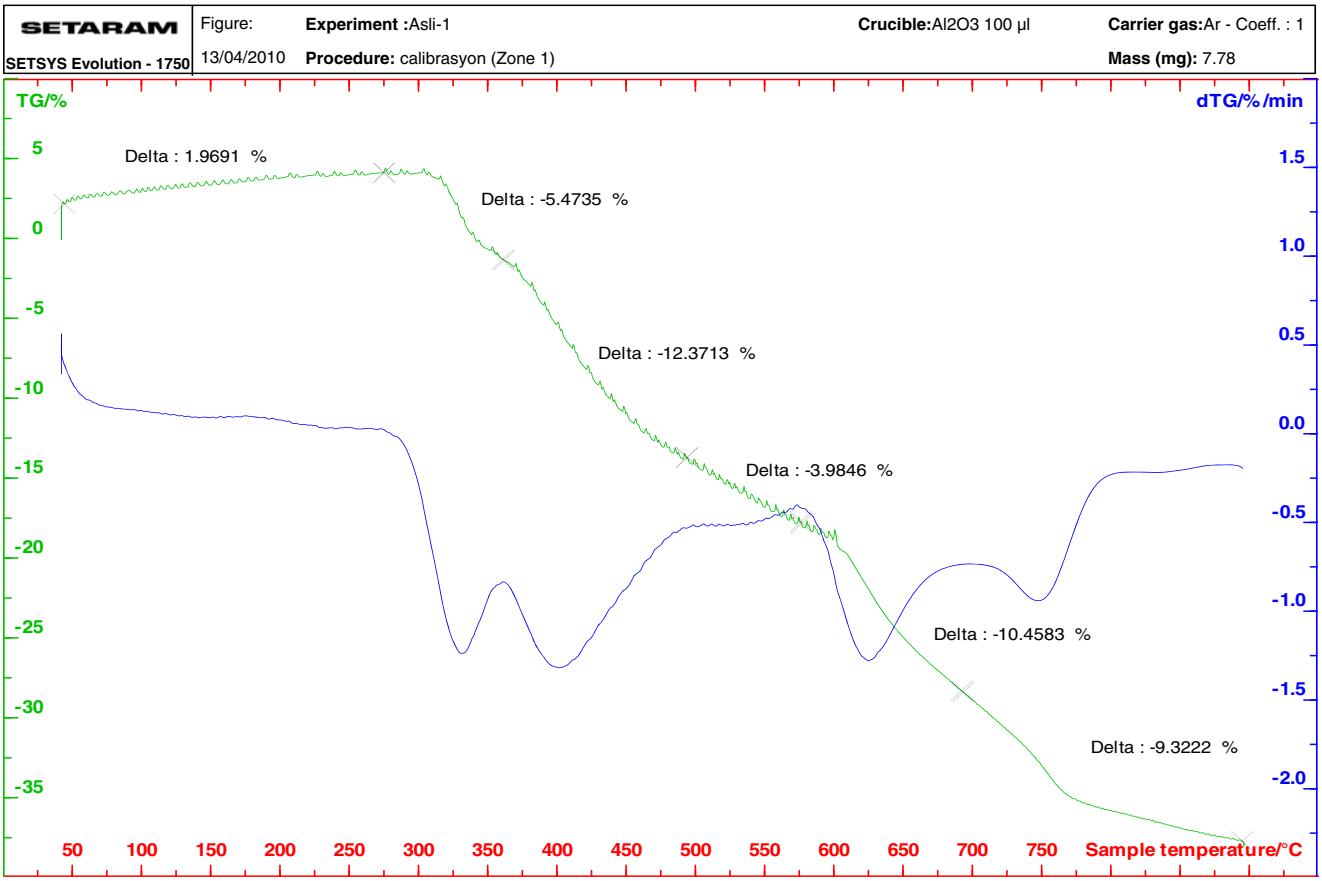

Fig. 7 TG/DTA diagram of [Fe (Saloph) L^5]

A: 1.049, **[Cr(Saloph)L^5];** Yield: % 54 (0.11 g), M.P.: 395 °C, FT-IR: 1,589 cm^{-1} (C = N), Color: Yellow, BM: 3.68, λ_{ems}: 301.73 nm, Fluorescence Intensity: 206.96, λ_{max}: 239 nm, A: 0.2327.

(For the complexes of L^5 ligand, the fluorescence intensities were measured at λ_{exc}: 227.12 nm).

Results and Discussion

The synthesis of novel metal chelation driven molecular pincers based on Salen type ligand substructures are described. Five novel Schiff base ligands, Fig. 1, have different chromophore groups. The oxygen bridged dimeric Salen type

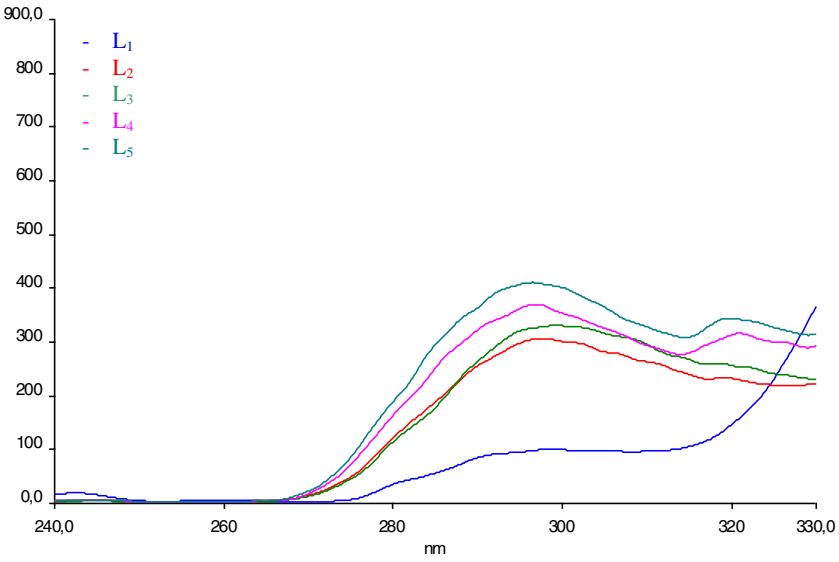

Fig. 8 Fluorescence intensities of ligands at 297 nm (1×10^{-6} M)

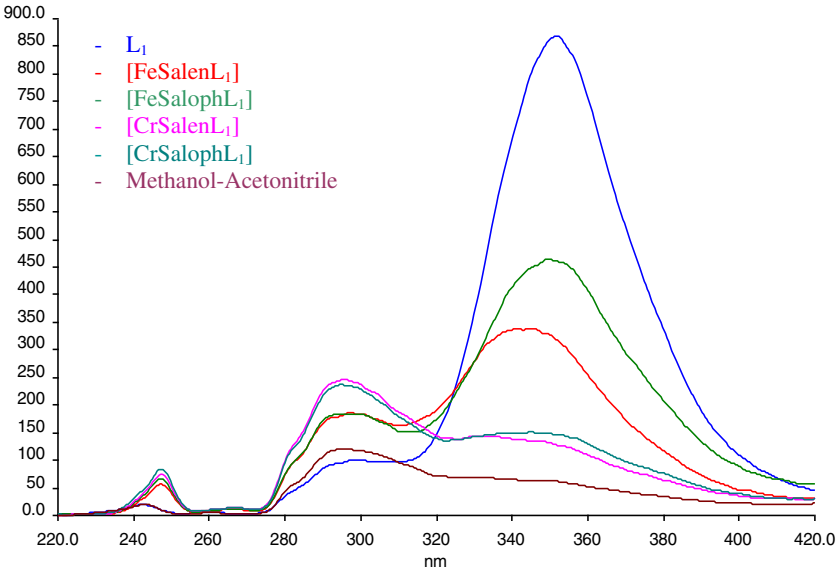

Fig. 9 Fluorescence intensities of L^1, [FeSalenL^1], [FeSalophL^1], [CrSalenL^1], [CrSalophL^1], methanol-acetonitrile solvent mixture at 355 nm (1×10^{-6} M)

complexes [{FeSalen}$_2$O], [{FeSaloph}$_2$O], [{CrSalen}$_2$O] and [{CrSaloph}$_2$O] can be called as ligand complexes. In this context we have performed the complexation of ligand complexes and fluorescent Schiff base ligands, as seen in Fig. 2. The resulting complexes are different tip Schiff base complexes bridged by carboxylate anions to the Fe(III) and Cr (III) centers. All compounds are stable at room temperature in solid state. Their structures are characterized and their fluorescence and absorbance properties are investigated.

FT-IR Spectra, ^{1}H-NMR Spectra, Magnetic Moment, Elemental Analysis and Thermal Analysis Interpretations of the Compounds

From FT-IR spectra of ligands L^n (n=1,2,3,4,5) and their complexes, it was seen that the vibrations of the imine -CH = N- groups of ligands L^n in order were observed at 1,677, 1,684, 1,678, 1,685, 1,675 cm^{-1}. After complexation with 'ligand complex' structures, these bands were shifted to lower frequencies has indicated that oxygen atoms of Schiff base ligands are coordinated with the 'ligand complex' structures (Table 1). The vibrations of imine -CH = N- groups for [Fe(Salen) L^1] is 1,631 cm^{-1}, [Fe(Saloph) L^1] is 1,603 cm^{-1}, [Cr(Salen) L^1] is 1,623 cm^{-1}, [Cr(Saloph) L^1] is 1,598 cm^{-1}, [Fe(Salen) L^2] is 1,624 cm^{-1}, [Fe(Saloph) L^2] is 1,601 cm^{-1}, [Cr(Salen) L^2] is 1,621 cm^{-1}, [Cr(Saloph) L^2] is 1,595 cm^{-1}, [Fe(Salen) L^3] is 1,621 cm^{-1}, [Fe(Saloph) L^3] is 1,581 cm^{-1}, [Cr(Salen) L^3] is 1,623 cm^{-1}, [Cr(Saloph) L^3] is 1,601 cm^{-1}, [Fe(Salen) L^4] is 1,589 cm^{-1}, [Fe(Saloph) L^4] is 1,581 cm^{-1}, [Cr(Salen) L^4] is 1,597 cm^{-1}, [Cr(Saloph) L^4] is 1,530 cm^{-1}, [Fe(Salen) L^5] is 1,628 cm^{-1}, [Fe(Saloph) L^5] is 1,576 cm^{-1}, [Cr(Salen) L^5] is 1,624 cm^{-1}, [Cr(Saloph) L^5] is 1,589 cm^{-1}. For the ligands the bands between 2,875 and 3,047 cm^{-1} assigned to the carboxylate -OH group vibrations. The bands at

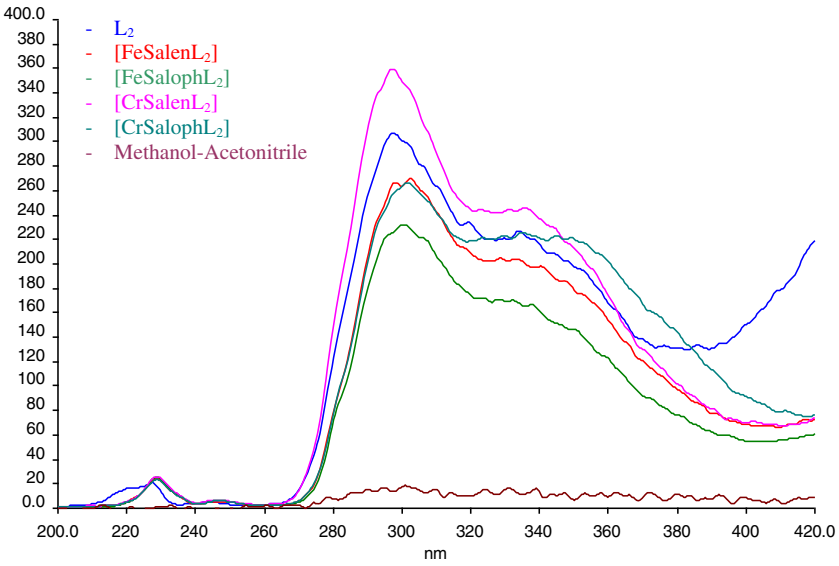

Fig. 10 Fluorescence intensities of L^2, [FeSalenL^2], [FeSalophL^2], [CrSalenL^2], [CrSalophL^2], methanol-acetonitrile solvent mixture at 299 nm (1×10^{-6} M)

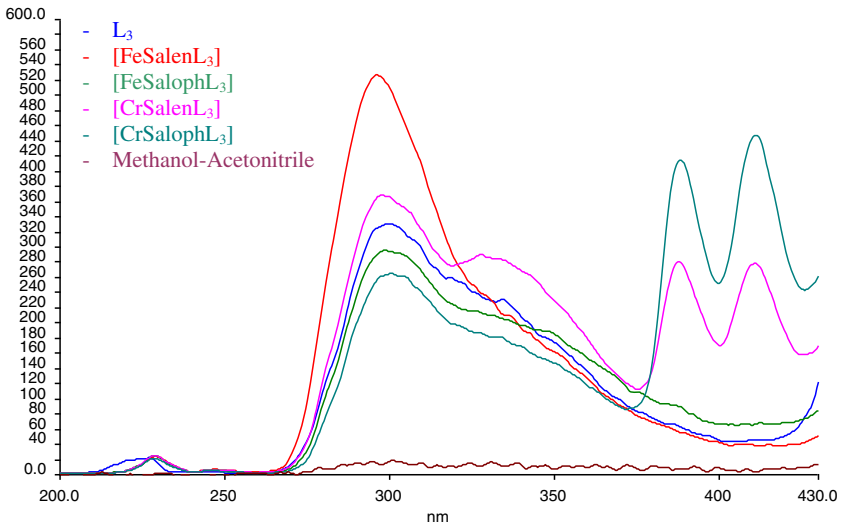

Fig. 11 Fluorescence intensities of L^3, [FeSalenL^3], [FeSalophL^3], [CrSalenL^3], [CrSalophL^3], methanol-acetonitrile solvent mixture at 299 nm (1×10^{-6} M)

1,288, 1,288, 1,288, 1,291, 1,291 cm^{-1} for the ligands were assigned to -C = O groups shifted due to the coordination of [Fe(Salen)], [Fe(Saloph)], [Cr(Salen)] and [Cr(Saloph)] with COO^- groups to 1291, 1295, 1313, 1296, 1301. These FT-IR values are compatible with previous works [30, 31].

In order to identify the ligand structures the ^{1}H-NMR spectra were recorded in DMSO-d6. The signals in spectra of L^n ligands at δ=8.60, 8.81, 8.80, 8.55, 9.67 ppm chemical shifts correspond to single protons of -CH = N- azomethine *groups,* Fig. 3. For the complex structures because the Fe(III) and Cr(III) metals are paramagnetic ^{1}H-NMR spectra did not be taken. To identify the complex structures after FT-IR studies magnetic moments were measured at room temperature. On the basis of spectral evidence the dendrimeric low spin Fe(III) and Cr(III) cations have an approximately octahedral environment. The magnetic moment of [Fe(Salen)L^n], [Fe(Saloph) L^n], [Cr(Salen) L^n] and [Cr(Saloph) L^n] shows paramagnetic property with a magnetic susceptibility values, given in experimental part, respectively. It is seen that the [{FeSalen}$_2$O], [{FeSaloph}$_2$O], [{CrSalen}$_2$O] and [{CrSaloph}$_2$O] containing compounds are represented by the electronic structure of $t_2g^5eg^0$ and $t_2g^3eg^0$. The magnetic data for the [{FeSalen}$_2$O], [{FeSaloph}$_2$O], [{CrSalen}$_2$O] and [{CrSaloph}$_2$O] complexes show good harmony with the low spin d^5 and d^3 metal ion in an octahedral structure [31].

Elementel analyses were performed for the ligands 4-(phenanthrene-9-ilmethyleneamino)benzoic acid, L^4, and 4-(pyrene-1-ilmethylenaamino)benzoic acid, L^5. According to the analyses results, the found values are compatible with calculated values. For L^4; calculated (found) C 81.23 (81.05), H 4.61 (4.52), N 4.30 (4.22), O 9.86 (10.11), for L^5; calculated (found) C 82.52 (82.67), H 4.29 (4.52), N

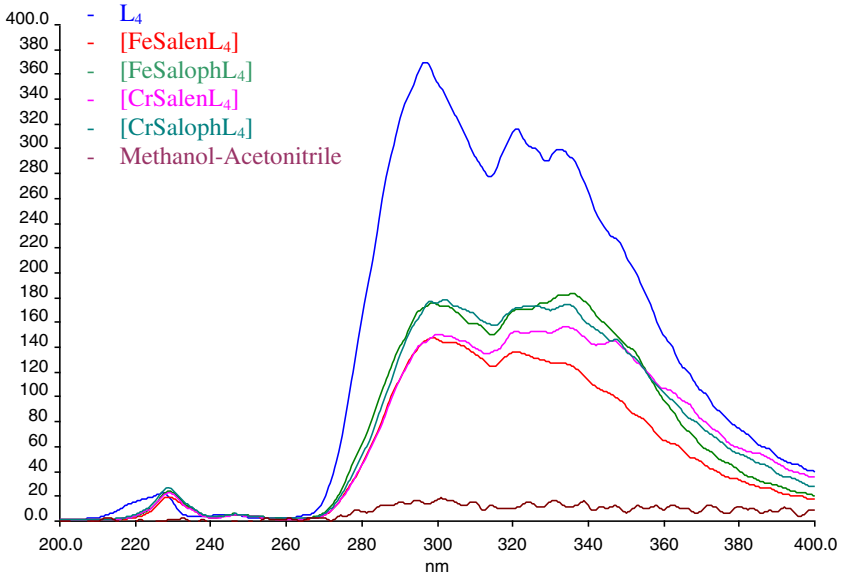

Fig. 12 Fluorescence intensities of L^4, [FeSalenL^4], [FeSalophL^4], [CrSalenL^4], [CrSalophL^4], methanol-acetonitrile solvent mixture at 299 nm (1×10^{-6} M)

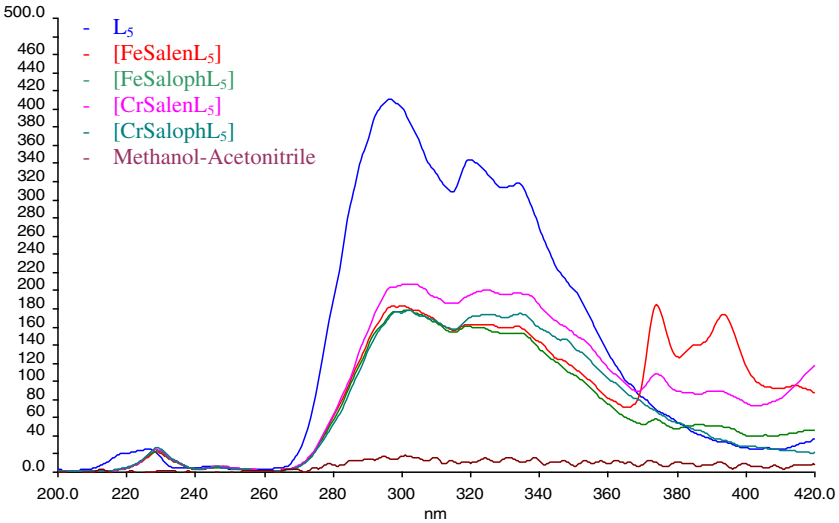

Fig. 13 Fluorescence intensities of L^5, [FeSalenL^5], [FeSalophL^5], [CrSalenL^5], [CrSalophL^5], methanol-acetonitrile solvent mixture at 299 nm (1×10^{-6} M)

4.01 (4.28), O 9.18 (8.52). The chosen complexes [Fe(Saloph)L^3], [Fe(Saloph)L^4], [Cr(Salen)L^4] and [Fe(Saloph)L^5] have also been thermally investigated and their plausible degradation schemes are presented in Figs. 4, 5, 6 and 7. For those complexes, thermal decomposition of the anhydrous [Fe(Saloph)] and [Cr(Salen)] complexes left from the ligands have started in the range of the first step 250–575 °C, the second step 475–690 °C and the final step 585–695 °C. The final decomposition products were metals and aromatic rings, pyrene, phenanthrene and anthracene. The observed weight losses for all ligands and complexes are in good harmony with the calculated values.

Table 2 Excitation wavelengts, emission wavelenghts and maximum fluorescence intensity values of the ligands and complexes

No	Compounds	λ_{eks} (nm)	λ_{ems} (nm)	Fluorescence intensity
1	L^1	242.71	351.22	867.72
2	[Fe(Salen)L^1]	242.71	342.81	336.62
3	[Fe(Saloph)L^1]	242.71	349.79	464.71
4	[Cr(Salen)L^1]	242.71	295.60	245.87
5	[Cr(Saloph)L^1]	242.71	295.60	236.49
6	L^2	227.55	297.65	306.82
7	[Fe(Salen)L^2]	227.55	300.20	264.46
8	[Fe(Saloph)L^2]	227.55	300.20	232.14
9	[Cr(Salen)L^2]	227.55	297.13	359.69
10	[Cr(Saloph)L^2]	227.55	301.73	266.77
11	L^3	227.56	300.63	329.84
12	[Fe(Salen)L^3]	227.56	296.11	526.96
13	[Fe(Saloph)L^3]	227.56	299.69	294.60
14	[Cr(Salen)L^3]	227.56	298.1	367.90
15	[Cr(Saloph)L^3]	227.56	300.71	265.26
16	L^4	227.77	296.87	369.79
17	[Fe(Salen)L^4]	227.77	299.18	147.62
18	[Fe(Saloph)L^4]	227.77	299.18	175.81
19	[Cr(Salen)L^4]	227.77	300.71	150.62
20	[Cr(Saloph)L^4]	227.77	300.20	176.06
21	L^5	227.12	296.87	410.42
22	[Fe(Salen)L^5]	227.12	299.18	182.6
23	[Fe(Saloph)L^5]	227.12	300.20	177.69
24	[Cr(Salen)L^5]	227.12	298.67	189.59
25	[Cr(Saloph)L^5]	227.12	301.73	206.96

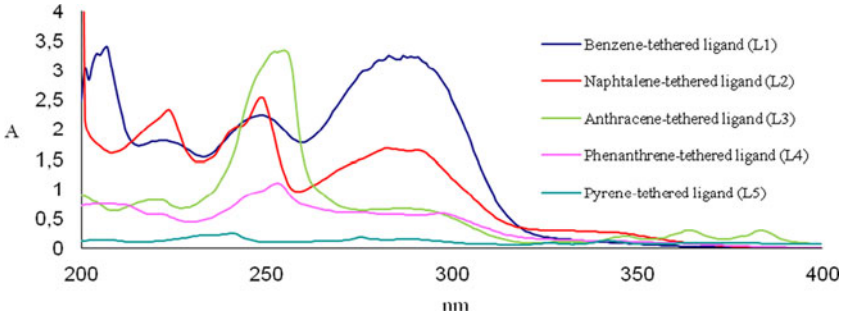

Fig. 14 Maximum absorbance sequence of ligands (1×10^{-5} M)

Fluorescence and Absorbance Investigation of Ligands and Complexes

All compounds were synthesized originally and all showed fluorescent property. Herein, fluorescent properties of chromophore-tethered Schiff base ligands and their complexes were measured in methanol-acetonitrile (4:3) medium with the concentration 1×10^{-6} M. As seen from Fig. 8 when all the ligands (1×10^{-6} M) excited at 297 nm, pyrene-appended one, L^5, shows the highest fluorescence and benzene-appended one, L^1, shows the lowest fluorescence. According to the conjugated π electron system fluorescence property changes. Increase of the aromatic groups in a system enhance the fluorescence. We proved that knowledge; at 297 nm the fluorescence intensities of ligands were observed as: $L^5 > L^4 > L^3 > L^2 > L^1$.

Schiff base compounds generally give weak emission bands. This is due to photoinduced electron transfer (PET) from lone pair of imine nitrogen to the photo-excited pyrene (or phenanthrene, anthracene, naphtalene, benzene) which leads to fluorescence quenching [32]. Herein, fluorescence intensities of L^1,L^4,L^5 with the concentration 1×10^{-6} M (at 355 nm for L^1, 299 nm for L^4 and L^5) are higher than their metal complexes. This is because of quenching effect of iron and chromium metals on chromophore groups. Ligands L^1,L^4, L^5 show more fluorescence than their complexes but interestingly, the other L^2 and L^3 ligands do not (Figs. 9, 10, 11, 12 and 13). In some fluorescence studies, somehow, it is seen Fe (III) and Cr(III) complexes show unexpected results [33–35]. The fluorescence intensity values at their excitation wavelengths of all compounds were given in Table 2.

The electronic absorption spectra of the free ligands and their metal complexes were recorded in solution at room temperature by UV–vis absorption spectroscopy. Absorbance studies were performed for all compounds between 200 and 800 nm. The solvent mixture were methanol-acetonitrile (4:3) with the concentration 1×10^{-5} M. The UV–vis absorption spectrum of all the compounds (1×10^{-5} M) exibits absorption bands between λ_{max}: 200–420 nm. As seen from Fig. 14, the decrease of aromatic groups in a system shifts maximum absorbance wavelenghts to the lowest energy regions. This shifts were resulted from π → π* ve n → π* electronic transitions between conjugated aromatic group and azomethine (CH = N) group in a system. Absorbances of all compounds at their maximum wavelengths were given in Table 3.

Table 3 Maximum absorbance values of ligand and complexes on UV-spectra

No	Bileşikler	λ_{maks} (nm)	Absorbans (A)
1	L^1	206	3.3474
2	[Fe(Salen)L^1]	219	2.903
3	[Fe(Saloph)L^1]	295	3.0874
4	[Cr(Salen)L^1]	200	1.4634
5	[Cr(Saloph)L^1]	200	1.8221
6	L^2	248	2.537
7	[Fe(Salen)L^2]	221	1.3493
8	[Fe(Saloph)L^2]	219	0.6474
9	[Cr(Salen)L^2]	222	0.9533
10	[Cr(Saloph)L^2]	221	1.8605
11	L^3	253	3.3119
12	[Fe(Salen)L^3]	254	1.0657
13	[Fe(Saloph)L^3]	250	1.0902
14	[Cr(Salen)L^3]	255	1.4216
15	[Cr(Saloph)L^3]	255	3.321
16	L^4	252	1.0836
17	[Fe(Salen)L^4]	250	0.5401
18	[Fe(Saloph)L^4]	254	1.5255
19	[Cr(Salen)L^4]	207	3.5425
20	[Cr(Saloph)L^4]	203	2.6077
21	L^5	241	0.24951
22	[Fe(Salen)L^5]	232	1.4992
23	[Fe(Saloph)L^5]	287	1.3726
24	[Cr(Salen)L^5]	232	1.049
25	[Cr(Saloph)L^5]	201	2.4721

Conclusion

In this context, fluorescent different tip Schiff base ligands are presented. All ligands contain a potential donor group capable of coordinating with the other ligand. We have

chosen [{FeSalen}$_2$O], [{FeSaloph}$_2$O], [{CrSalen}$_2$O], [{CrSaloph}$_2$O] as 'ligand complexes' because they can coordinate with the other ligand. These complexes are different tip Schiff base complexes bridged by carboxylate anions to the iron and chromium centers. Their structures were characterized by means of FT-IR Spectroscopy, ^{1}H-NMR Spectroscopy, Magnetic Susceptibility, Elementel Analsis, TG/DTA. The magnetic data for the complexes show good harmony with the d^5 and d^3 metal ion in an octahedral structure. Absorption and fluorescence properties were investigated by UV–vis Spectroscopy and Luminescence Spectroscopy.

Acknowledgments We thank the Scientific Research Projects Foundation of Selcuk University (Konya/TURKEY) (SUBAP-Grant Number 2010/09101052) for financial support of this work produced from a part of Aslıhan YILMAZ OBALI's MSc Thesis.

References

1. Abe AMM, Helaja J, Koskinen AMP (2006) Novel crown ether and Salen metal chelation driven molecular pincers. Org Lett: 4537–4540
2. Shiraishi Y, Tokitoh Y, Hirai T (2006) pH-and H2O-driven triple-mode pyrene fluorescence. Org Lett 8:3841–3844
3. Suzuki I, Ui M, Yamauchi A (2006) Pyrene-appended α-cyclodextrin as a fluorescent pH probe responding to a wide range. Anal Sci 22:655–657
4. Kumar M, Babu JN, Bhalla V (2010) Fluorescent chemosensor for Cu2+ ion based on iminoanthryl appended calix[4]arene. J Incl Phenom Macrocycl Chem 66:139–145
5. Lohr HG, Vogtle F (1985) Chromo-and fluoroionophores. A new class of dye reagents. Acc Chem Res 18:65
6. Fabrizzi L, Poggi A (1995) Sensors and switching from supramolecular chemistry. Chem Soc Rev 95:197
7. Czarnik AW (1994) Chemical communication in water using fluorescent chemosensors. Acc Chem Res 27:302
8. de Silva AP, de Silva SA (1986) Fluorescent signalling crown ethers; 'switching on' of fluorescence by alkali metal ion recognition and binding *in situ*. J Chem Soc Chem Commun 23:1709
9. Richard AB, Calle E, de Silva AP, de Silva SA, Gunaratne HQN, Habib-Jiwan JL, Peiris SLA, Rupasinghe RADD, Samarasinghe TKSD (1992) Luminescence and charge transfer. Part 2. Aminomethyl anthracene derivatives as fluorescent PET (photoinduced electron transfer) sensors for protons. J Chem Soc Perkin Trans 2 (9):1559
10. de Silva AP, Gunaratne HQN, Gunnlaugsson McCoy CP, Maxwell RS, Rademacher JT, Rice TE (1996) Photoinduced electron transfer systems with switchable luminescence output. Pure Appl Chem 48:1443
11. de Silva AP, Gunaratne HQN, Gunnlaugsson T, Huxley AJM, McCoy CP, Rademacher JT, Rice TE (1997) Signaling recognition events with fluorescent sensors and switches. Chem Rev 97:1515
12. Kubo K, Ishige R, Kato N, Yamamoto E, Sakurai T (1997) Synthesis and complexation behavior of N, N′-bis(1- naphthylmethyl)-1,4,10,13-tetraoxa-7,16-diazacyclo-octadecane). Heterocycles 45:2365
13. Kubo K, Kato N, Sakurai T (1997) Synthesis and complexation behavior of diaza-18-crown-6 carrying two pyrenylmethyl groups. Bull Chem Soc Jpn 70:3041
14. Kubo K, Ishige R, Sakurai T (1998) Synthesis and complexation behavior of N, N′-bis (9-anthrylmethyl)-1, 4, 10, 13-tetraoxa-7, diazacyclooctadecane. Heterocycles 48:347
15. Kubo K, Ishige R, Sakurai T (1999) Synthesis and complexation behavior of *N*-(1-naphthylmethyl)-1,4,7,10,13-pentaoxa-16- azacyclooctadecane. Talanta 48:181
16. Shi Q, Cao R, Li X, Luo J, Hong M, Chen Z (2002) Syntheses, structures, electrochemistry and magnetic properties of chain-like dicyanamide manganese(III) and iron(III) complexes with salen ligand. New J Chem 26:1397–1401
17. Darensbourg D, Ortiz CG, Billodeaux DR (2004) Synthesis and structural characterization of iron(III) salen complexes possessing appended anionic oxygen donor ligands. Inorg Chim Acta 357:2143–2149
18. Roy P, Dhara K, Chakroborty J, Nethaji M, Banerjee P (2007) Synthesis and crystall structure of an iron (II) dimeric complex. Indian J Chem 46A:1947–1950
19. Tonami H, Uyama H, Oguchi T, Higashimura H, Kobayashi S (1999) Synthesis of a soluble polyphenol by oxidative polymerization of bisphenol-A using iron-salen complex as catalyst. Polym Bull 42:125–129
20. Barone G, Silvestri A, La Manna G (2005) DFT computational study on FeIII-N, N′-ethylene-bis(salicylideneiminato) derivatives. Mol Struct THEOCHEM 715:79–83
21. Wollmann RG, Hendrickson DN (1978) Reaction of mu.-oxobridged iron(III) complexes with organic acids: a characterization of the products. Inorg Chem 17(4):926–930. doi:10.1021/ic50182a026
22. Koc ZE, Ucan HI (2007) Complexes of iron(III) salen and saloph Schiff bases with bridging 2,4,6- *tris* (2,5- dicarboxyphenylimino-4-formylphenoxy)-1,3,5-triazine and 2,4,6- *tris* (4-carboxyphenylimino-4′-formylphenoxy)-1,3,5-triazine. Transit Met Chem 32:597–602. doi:10.1007/s11243-007-0213-7
23. Juturu V, Komorowski JR (2003) Chromium supplements, glucose, and insulin responses. Am J Clin Nutr 78:192–193
24. Srinivasan K, Michaud PJ, Kochi K (1986) Epoxidation of olefins with cationic (salen) manganese (III) complexes. The modulation of catalytic activity by substituents. J Am Chem Soc 108:2309–2320. doi:10.1021/ja00269a029
25. Samsel EG, Srinivasan K, Kochi JK (1985) Mechanism of the chromium-catalyzed epoxidation of olefins. Role of oxochromium (V) cations. J Am Chem Soc 107:7606–7617. doi:10.1021/ja00311a064
26. Yoon H, Burrows CJ (1988) Catalysis of alkene oxidation by nickel salen complexes using sodium hypochlorite under phase- transfer. J Am Chem Soc 110:4087–4089. doi:10.1021/ja00220a086
27. Luts T, Frank R, Suprun W, Fritzsche S, Hey-Hawkins E (2007) Epoxidation of olefins catalyzed by novel Mn(III) and Mo(IV) - Salen complexes immobilized on mesoporous silica gel part II: study of the catalytic epoxidation of olefins. H Papp J Mol Catal A Chem 273:250–258. doi:10.1016/j.molcata.2007.04.010
28. Kopel P, Sindelar Z, Klicka R (1998) Complexes of iron (III) salen and saloph Schiff bases with bridging dicarboxylic and tricarboxylic acids. Transit Met Chem 23:139–142. doi:10.1023/A:1006990925318
29. Gembicky M, Boca R, Renz F (2000) A heptanuclear Fe_II/–Fe_III/system with twelve unpaired electrons. Inorg Chem Commun 3:662–665. doi:10.1016/S1387-7003(00)00160-X
30. Koc ZE, Ucan HI (2008) Complexes of Iron(III) and Chrom(III) Salen and Saloph Schiff Bases with Bridging 2,4,6-tris(4-nitrophenylimino-4′-formylphenoxy)-1,3,5-triazine. J Macromol Sci A 45(12):1072–1077. doi:10.1080/10601320802458087
31. Kopel P, Sindelar Z, Biler M, Klicka R (1998) Complexes of iron (III) salen and saloph Schiff bases bridges by dicarboxylic acids. Pol J Chem 72(9):2060–2066
32. Kubo K, Ishige R, Sakurai T (1999) Complexation and fluorescence behavior of diazacrown ether carrying two anthryl pendants. Talanta 49:339

33. Mao J, Wang L, Dou W, Tang X, Yan Y, Liu W (2007) Tuning the selectivity of two chemosensors to Fe (III) and Cr (III). Org Lett 9 (22):4567–4570
34. Sahoo SK, Bera RK, Baral M, Kanungo BK (2007) Excited state intramolecular proton transfer (ESIPT) in a dioxotetra-amine derived schiff base and its complexation with Fe (III) and Cr (III). J Photochem Photobiol A Chem 188:298–310
35. Lin C-T, Bottcher W, Chou M, Creutz C, Sutin N (1976) Mechanism of the quenching of the emission of substituted polypyridineruthenium (II) complexes by iron (III), chromium (III), and europium (III) ions. J Am Chem Soc 98:21